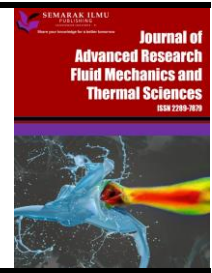




# Journal of Advanced Research in Fluid Mechanics and Thermal Sciences

Journal homepage:  
[https://semarakilmu.com.my/journals/index.php/fluid\\_mechanics\\_thermal\\_sciences/index](https://semarakilmu.com.my/journals/index.php/fluid_mechanics_thermal_sciences/index)  
ISSN: 2289-7879



## Stretched Meshing in a 2D Computational Domain with Elbow Edges for CFD Applications

Gancang Saroja<sup>1</sup>, Sugeng Rianto<sup>1</sup>, Abdurrouf<sup>1</sup>, Setyawan Purnomo Sakti<sup>1</sup>, Muhammad Nurhuda<sup>1,\*</sup>

<sup>1</sup> Department of Physics, Faculty of Sciences, Brawijaya University, Malang, East Java, Indonesia

ARTICLE INFO	ABSTRACT
<p><b>Article history:</b> Received 10 October 2023 Received in revised form 25 March 2024 Accepted 4 April 2024 Available online 30 April 2024</p> <p><b>Keywords:</b> Mesh generation; structured mesh; elbow boundary edges; stretching; quality of mesh</p>	<p>Mesh generation is critical for obtaining accurate and detailed solutions to mesh-based numerical problems, particularly when capturing specific information within a designated area of the domain. While structured meshes offer consistency, their uniform resolution limits their ability to achieve this. Mesh stretching offers a solution by introducing non-uniform element sizes based on an analytical relationship while preserving the original mesh structure. The objective of this study is to create a hybrid mesh model that leverages the strengths of both structured and stretched meshes. A 2D rectangle with elbow edges serves as the domain. To address the requirements of CFD applications, the domain is refined by increasing element density near the boundaries and corners. Skewness, aspect ratio, and element quality are then assessed to determine the overall mesh quality. The results demonstrate that stretching the structured mesh produced a mesh with quality that meets CFD domain standards.</p>

### 1. Introduction

In computational fluid dynamics (CFD) simulations, computational domains with non-linear edge boundaries present a particularly interesting and challenging problem to study. Identifying bend paths, as described by Hashim *et al.*, [1], and wall corners is of crucial interest as these sites host various significant physical phenomena. When fluid flows through a curved path, centrifugal forces generate pressure and velocity differences across the path, as documented in previous studies [2,3]. This phenomenon carries valuable information about physical quantities, making it essential for detailed observation in both simulations and experiments, as demonstrated by Kumar *et al.*, [4] and Cao *et al.*, [5]. Consequently, constructing a suitable computational domain becomes essential to accurately capture and represent this information.

In the numerical solution of mesh-based CFD problems, non-homogeneous element distributions within the computational domain are widely used. This diversity in element distribution adapts to the varying flow properties in different parts of the domain. For example, certain areas might exhibit turbulent vortices, while others experience laminar and steady flow. As a result, various methods

\* Corresponding author.

E-mail address: [mnurhuda@ub.ac.id](mailto:mnurhuda@ub.ac.id)

<https://doi.org/10.37934/arfmts.116.2.4150>

have been developed to construct suitable meshes for the computational domain, including the stretched mesh method.

The stretched mesh method generates meshes with varying element sizes based on an analytical relationship between elements within the domain. This allows elements to adapt in size, growing or shrinking, according to either their order or a combination of order and other patterns, as explored in the study by Llorente *et al.*, [6]. Furthermore, the underlying analytical relationship governing cell size can be linear or nonlinear, offering flexibility for different scenarios.

The stretched mesh method has found applications in climate analysis, demonstrating its efficiency for regional simulations as shown by Qian *et al.*, [7]. Their study employed a 2D square domain with geometric symmetry along both  $x$  and  $y$  axes in the Cartesian coordinate system. This symmetry simplifies the formulation of analytical relationships between elements within the mesh. To enable focused observation on a specific area, a buffer zone of smaller elements was implemented around the domain's center.

CFD simulations often involve complex geometries like rectangles with sharp turns and corners, making it difficult to maintain a consistent structured mesh throughout the domain. One approach, the multi-block scheme by Ali *et al.*, [8,9], tackles this by dividing the domain into simpler sub-domains. While effective, this method requires careful decomposition, which can be time-consuming and complex. Another option is the advancing extraction method (AEM) by Zhang and Jia [10], which can directly generate structured meshes for complex 2D geometries. However, this method still produces meshes with uniform element sizes within each subdomain, limiting its ability to adapt to varying flow characteristics.

This research investigates the potential synergy of combining structured mesh formation and mesh stretching methods for computational domain models with elbow-shaped boundaries. We expect that this exploration could pave the way for further advancements and development in this field.

Our paper is organized as follows: Section 2 discusses the methods employed, encompassing the mapping of the computational domain, decomposition of the domain into subdomains, implementation of structured meshes within each subdomain, stretching the mesh in each subdomain, and evaluation of mesh quality. In Section 3, we present the results of our work, which are classified as low, medium, and high based on their resolution. Finally, the conclusion of our work is disclosed in Section 4.

## 2. Methodology

To effectively adapt meshes to the presence of elbow-shaped edges in 2D domains, we have implemented a five-stage approach. Each stage plays a critical role in constructing a high-quality stretched mesh; therefore, we will elaborate on each one in detail.

### 2.1 Map of the Computational Domain

Applying the mesh stretching method to domains with numerous corners presents unique challenges. To tackle this complexity, we begin with a simplified domain featuring a single elbow and its boundary, resulting in six initial corners (Figure 1(a)). This geometric shape mirrors the bending domain model used by Zhang and Jia [10]. We define the computational domain by mapping physical coordinates  $(x, y)$  within the 2D plane, with the main computational domain (level 0) serving as the foundation for subsequent decomposition.

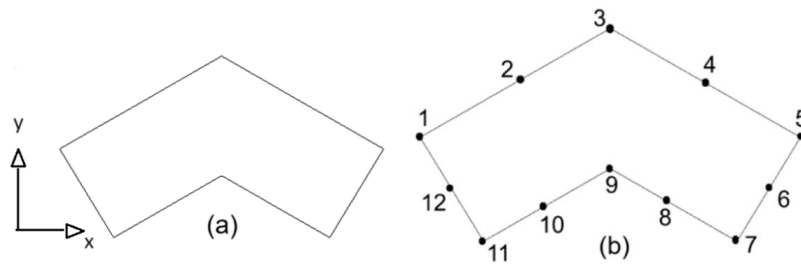


**Fig. 1.** (a) Domain in physical coordinates and (b) in computational coordinates with control points at the domain boundary

## 2.2 Decomposition of the Level 0 Domain into Subdomains

The initial step in the decomposition process is to position control points along the domain boundaries. These points can be placed at any location on the boundary, either along straight sections or at corners. To distinguish their roles, we categorize them into three types: convex points, concave points, and flat points. These designations are based on their positions relative to the domain boundary, as illustrated in Figure 1(b). Points situated on the straight sections of the boundary are classified as flat points (points 2, 4, 6, 8, 10, and 12). Those positioned at corners where the angle is less than  $180^\circ$  are identified as convex points (points 1, 3, 5, 7, and 11). Finally, a point situated in a corner with an angle exceeding  $180^\circ$  is designated as a concave point (point 9). Following control point placement, the next stage involves decomposing the level 0 domain into subdomains, also known as level 1 domains.

## 2.3 Implementation of a Structured Mesh in Each Subdomain

After completing the decomposition stage, all subdomains are meshed using a structured approach. The first step involves determining the desired resolution, wherein the element size, or element length interval, is calculated by dividing the length of a domain boundary side by the resolution value. In this work, quadrilateral elements are employed for the structured mesh model. For ease of comparison, three established resolution levels are utilized: low (L), medium (M), and high (H). These categories align with how resolution has been classified in previous studies, with a resolution of  $41 \times 41$  representing the simplest category, as employed by Gupta and Kalita [11]. Although there is no specific classification for higher resolutions, we adopt three values based on the distribution of various resolution values described by Marchi *et al.*, [12]. For the low-resolution case, a mesh size of  $41 \times 41$  will be utilized, followed by  $80 \times 80$  and  $129 \times 129$  as representatives of medium and high resolutions, respectively.

## 2.4 Stretching the Mesh in Each Subdomain

In the fourth stage, a specific target area within the subdomain undergoes stretching. This stretching process, implemented in the physical coordinate system ( $x, y$ ), results in the modification of the size of elements. The interval length changes in both the horizontal ( $x$ ) and vertical ( $y$ ) directions, following a specific analytical relationship between elements. To measure this change, we introduce the total strain level denoted by  $R$ . This value signifies the ratio between the largest and smallest element intervals within the target area. Specifically, in the  $x$ -direction,  $R$  must satisfy the following conditions:

$$R = \frac{\Delta x_{\max}}{\Delta x_{\min}} > 1 . \quad (1)$$

To further refine the mesh adaptation, we introduce a local strain rate parameter, denoted by  $r_i$ . This value represents the ratio of an element's size to its nearest neighbor's size. It plays a critical role in determining the analytical relationship that governs the stretching process, which is expressed as follows:

$$r_i = \frac{\Delta x_i}{\Delta x_{i-1}} = \frac{x_{i+1} - x_i}{x_i - x_{i-1}} \quad (2)$$

where  $\Delta x$  represents the interval length in the  $x$ -direction of the physical coordinate system, and  $i$  is the integer number (1, 2, 3, ...) that reflects the position of elements. Similar conditions apply to the  $y$ -direction coordinates. It should be noted that stretching will be concentrated in a target area near the domain boundaries and corners. This choice aligns with the well-documented occurrence of vortices near fluid boundaries, as noted by Moffatt [13]. Furthermore, the flow velocity in the boundary or wall region depends heavily on the specific boundary conditions, necessitating detailed observation in these areas.

### 2.5 Evaluating Mesh Quality

The quality of a simulation's mesh directly impacts the quality of its results. A high-quality mesh typically adheres to two key criteria: minimal skewness, implying minimal changes in the area between adjoining elements, and an appropriate aspect ratio, ensuring sufficient resolution in information-dense regions. As Lintermann [14] point out, element shape, defined by skewness and aspect ratio, is the primary determinant of mesh quality.

In a quadrilateral element, the aspect ratio measures the relative lengths of its sides, expressed as the ratio of its longest side to its shortest. Figure 2 depicts a square mesh element with various aspect ratios. Generally, an aspect ratio closer to 1 indicates a better quality mesh. For highly accurate results, the recommended range is between 0.2 and 5.

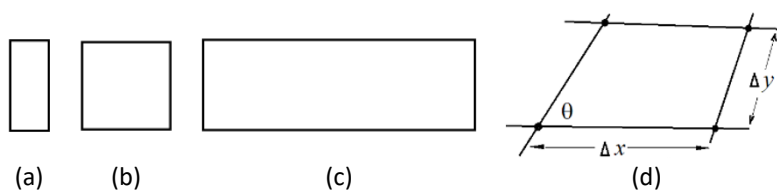


**Fig. 2.** (a) Square elements with a low aspect ratio, (b) =1 aspect ratio, and (c) a high aspect ratio (d) Skewness of a quadrilateral element

Skewness, also known as mesh distortion, reflects the deviation of an element's shape from a perfect rectangle. This is measured by the angle between its edge lines. An element with zero skewness, denoted by  $\theta \approx 90^\circ$ , is perfectly orthogonal. However, for practical applications, skewness values within a certain range, like  $\theta \leq 45^\circ$  or  $\theta \geq 135^\circ$ , are acceptable. Generally, skewness is quantified on a scale of 0 to 1, where 0 represents a perfect rectangle and higher values indicate increasing distortion. According to ANSYS [15], elements with lower skewness values possess higher quality. Figure 2(d) illustrates the angle of inclination for quadrilateral elements, highlighting the impact of skewness.

Beyond aspect ratio and skewness, another critical parameter for mesh quality is element quality. For quadrilateral elements, this represents the ratio of their area to the sum of squared edge lengths, as shown in Eq. (3) with value of  $c = 4$ . Ranging from 0 to 1, element quality acts as a combined metric. A value of 1 signifies a highly desirable element, similar to a perfect square or cube. Conversely, a value of 0 indicates a severely distorted element, potentially with zero or negative volume. Table 1 summarizes standard quality parameter values and their classifications. For reference, the mesh construction and analysis were conducted using ANSYS software.

$$Q = c \left[ \frac{\text{Area}}{\sum(\text{Edge length})^2} \right] \tag{3}$$

**Table 1**

Standard values of the mesh quality parameters for aspect ratio and skewness

Parameter	Standard Value						
Aspect ratio [14]	0.2 – 5.0						
Skewness [15]	equilateral	Excellent	good	fair	poor	bad	degenerate
	0	0 – 0.25	0.25 – 0.50	0.50 – 0.75	0.75 – 0.90	0.90 - <1	1

### 3. Results and Discussions

#### 3.1 Results of the Decomposition Process

Referring to Figure 3, the main domain (level 0) is divided into two subdomains, A and B. To ensure the consistent construction of a structured mesh using quadrilateral elements, each subdomain requires four sides, necessitating at least four control points serving as turning points. This corresponds with prior research of Zhang and Jia [10], which highlights that a minimum of four turning points is necessary during decomposition for domains with various shapes to achieve a structured mesh. Figure 3 illustrates that the decomposition process involves connecting convex point (3) and concave point (9), resulting in the "adjunction line," which serves as the boundary separating the two subdomains. This line acts as a constraint for both subdomains A and B, with points along it being shared between them. These newly formed subdomains, A and B, are designated as "level 1 domains" since they represent the first-stage decomposition of the level 0 domain.

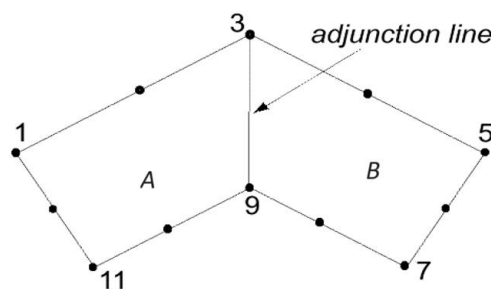


**Fig. 3.** Sketch the adjunction lines on the level 0 domain that will produce subdomains A and B

### 3.2 Evaluation of the Structured Mesh Model

We employ structured meshes with three varying resolution levels (low, medium, and high) applied to the level 1 domain, as shown in Figure 4. Each mesh consists of elements with interval lengths uniformly distributed across each subdomain boundary. It is important to note that these lengths vary based on the chosen resolution. The impact of the elbow is noticeable in areas adjacent to the subdomain boundaries. This occurs because the decomposition process generates subdomains with uneven side lengths. As a result, the equilateralness of elements diminishes, particularly near these boundaries, and this effect becomes more pronounced with higher resolutions (see Figure 4(c)). In this figure, the resolution around the subdomain boundaries appears notably dense.

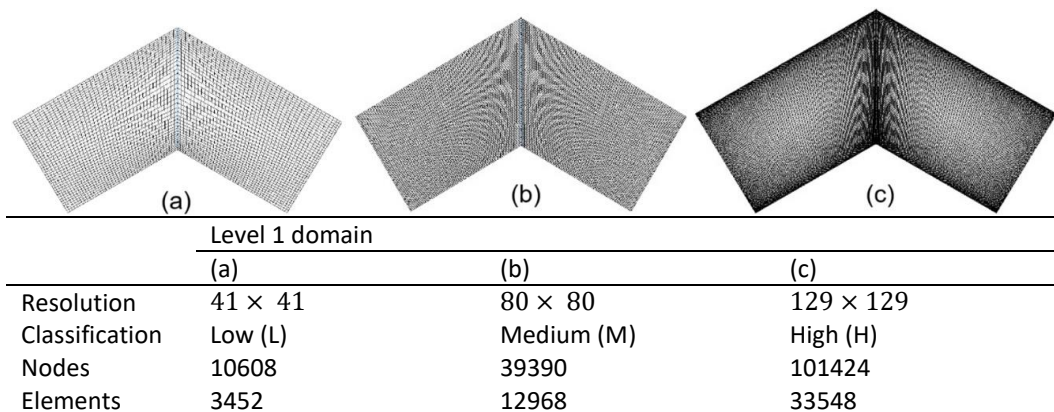


**Fig. 4.** Regular structured meshes in (a) low, (b) medium, and (c) high-classification

To evaluate the level 1 domain mesh quality, we analyse the distributions of skewness values, aspect ratios, and element quality. Table 2 illustrates that the minimum skewness value decreases in the high-resolution domain, indicating an improvement in element skewness with higher resolution. Interestingly, the maximum skewness value remains constant at 0.3309 across all resolution categories. While aspect ratios show minimal variations without a clear pattern across resolutions, element quality presents a different scenario. The minimum value moderately decreases at high resolution, but the maximum value remains fixed at 0.9996. This suggests that, despite a relatively small change, element quality might slightly decrease at high resolution. This strongly suggests that increasing mesh resolution within the same level 1 domain does not significantly impact the overall quality of the structured mesh.

**Table 2**

Distribution of mesh quality values for level 1 domain with L, M, and H classifications, without stretching

Parameter	Resolution Classification					
	L		M		H	
	Min	Max	Min	Max	Min	Max
Skewness	0.0038	0.3309	0.0027	0.3309	0.0026	0.3309
Aspect ratio	1.0005	1.8350	1.0004	1.8201	1.0068	1.8396
Elements quality	0.7908	0.9996	0.7895	0.9996	0.7882	0.9996

### 3.3 Evaluation of Stretch Mess

The next stage involves applying stretching to the three structured meshes, as illustrated in Figure 5. This process modifies the sizes of the element intervals across each domain side. Notably, the stretched mesh system features a consistent relationship between the sizes of neighboring intervals, resulting in a constant local stretching factor  $r$ . This relationship between  $r$  and the total stretching applied to one domain side  $R$  can be expressed as follows

$$R = r^l, \tag{4}$$

where  $l$  is an integer representing the relation index between the total stretching and the local stretching. The value of  $l$  is set to 5 to meet the algebraic requirements outlined by Qian *et al.*, [7].

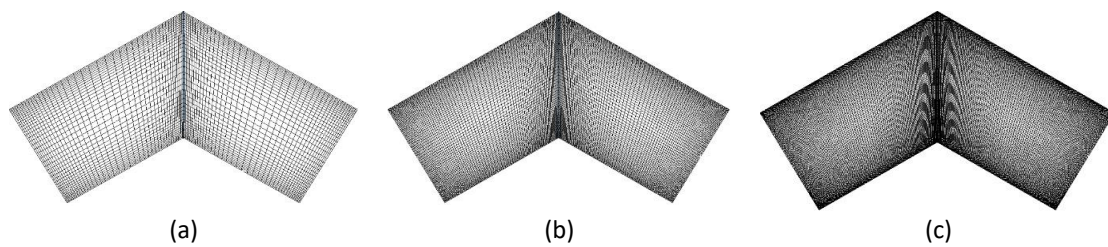


**Fig. 5.** The structured mesh for (a) L, (b) M, and (c) H-resolution with stretching

Table 3 summarizes the quality test results for the stretched mesh. Similar to the unstretched mesh, the distribution of element skewness remains consistent. While the range of maximum and minimum values shows no significant alterations, there is a slight decrease in minimum skewness with higher resolutions. This suggests that mesh stretching within the same domain has a minimal impact on overall skewness. However, stretching significantly increases the maximum aspect ratio, jumping from approximately 1 to 8. This behavior arises from the stretching process selectively shrinking element intervals in specific areas to enhance resolution. As a result, elements near the subdomain center enlarge, while those near the edges shrink, leading to a higher aspect ratio. Additionally, stretching influences element quality, reducing the minimum value compared to the unstretched mesh. This implies an increase in the number of non-equilateral elements following the stretching process.

**Table 3**

Distribution of mesh quality parameter values for level 1 domains in L, M, and H resolutions with stretching

Parameter	Resolution Classification					
	L		M		H	
	min	max	min	max	min	max
Skewness	0.0036	0.3309	0.0025	0.3309	0.0015	0.3309
Aspect ratio	1.0013	8.5624	1.0003	8.9974	1.0003	8.8600
Elements quality	0.2302	0.9998	0.2194	0.9997	0.2227	0.9998

To comprehensively evaluate the effect of stretching on mesh quality, we conducted an analysis of the average values of skewness, aspect ratio, and element quality parameters. Figure 6 provides a comparison of these qualities across resolutions. In the level 1 domain, stretching has minimal impact on skewness at any resolution level. However, it significantly affects the aspect ratio, increasing the average value from roughly 1.4 to 2.1 across all resolutions.

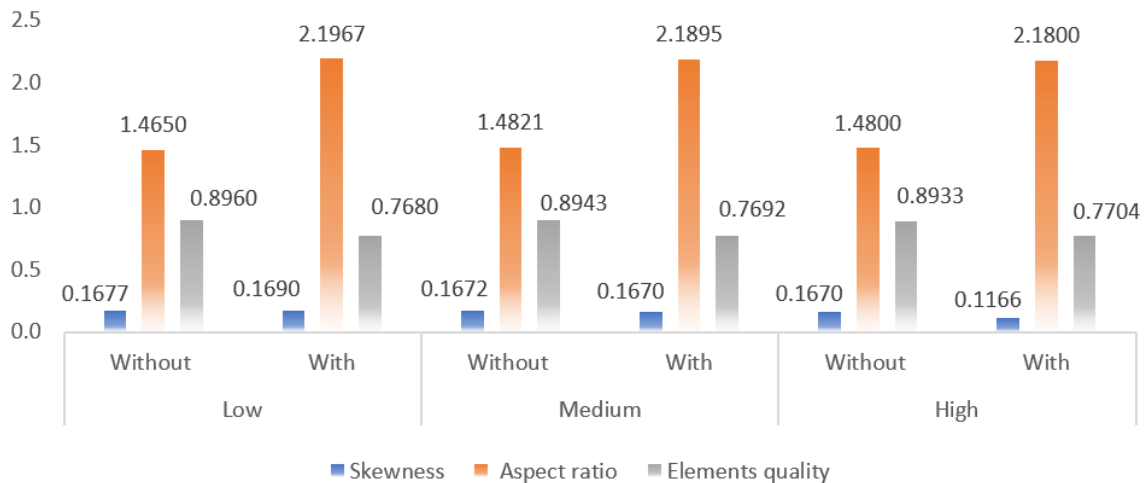


**Fig. 6.** Comparison of average skewness, aspect ratio, and element quality values of mesh in level 1 domain with and without stretching

The suitability of the three stretched meshes for CFD applications can be evaluated by comparing their mesh quality values with standard ranges (Table 1). The skewness values of these meshes (0.1166, 0.1670, and 0.1690) all fall within the excellent classification range. The average aspect ratios of the three resolutions (2.1800, 2.1895, and 2.1967) also lie within the recommended range of 0.2 to 5.0. Similarly, the average element quality values for the three resolutions (0.7680, 0.7692, and 0.7704) are all close to 1 on a scale of 0 to 1, indicating good quality. Based on these assessments, all resolutions of the stretched meshes are considered suitable for the CFD computational domain.

To demonstrate the practical advantages of our stretched mesh models, we applied one to a fluid flow simulation. Figure 7 and Figure 8 compare two scenarios: a simulation with a non-stretched mesh and one with our stretched mesh. Both were set up as laminar flow simulations with a Reynolds number of 1000. The fluid enters the domain from the left inlet at 1 m/s in the positive x-direction and exits through the right outlet, as shown in Figure 1(a).

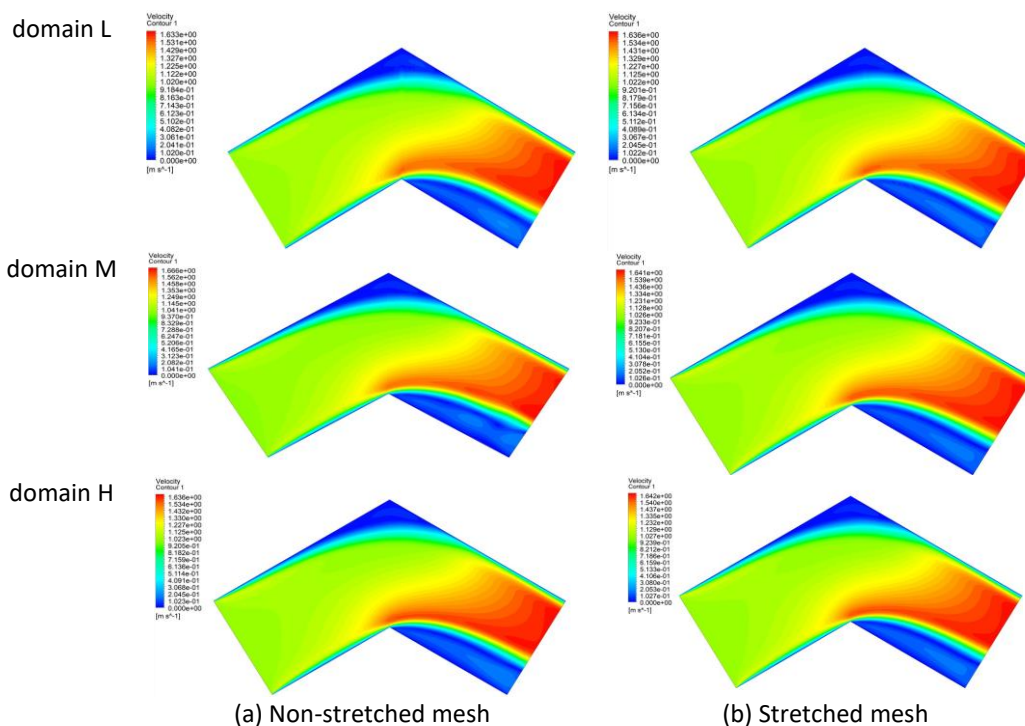


**Fig. 7.** Contour plots of fluid velocity inside the domain

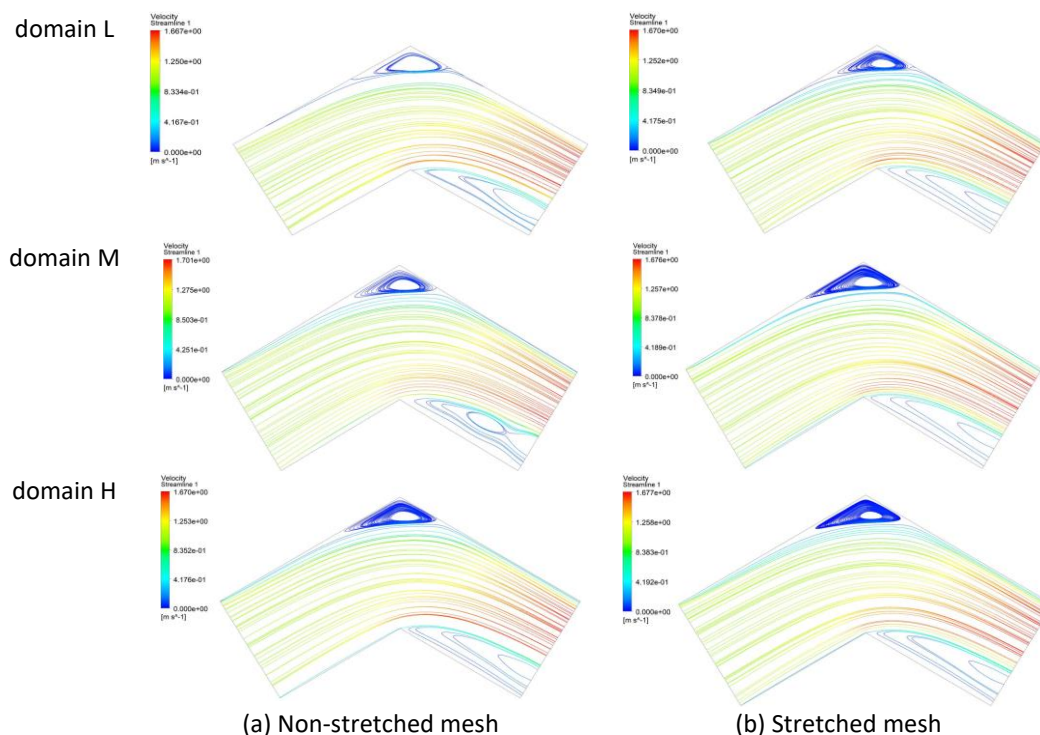


**Fig. 8.** Streamline plots of fluid velocity inside the domain

Our simulations show that stretching the mesh, regardless of the resolution parameter used, creates a denser concentration of vortices near the corner. This pattern is visible even at low resolutions, a phenomenon absent in unstretched meshes. These observations strongly support the effectiveness of mesh stretching in this study, though further detailed investigations are necessary and beyond the scope of this work.

#### 4. Conclusions

In this work, we successfully apply the stretched meshing method to construct structured meshes for domains with elbow boundaries. This approach achieves higher resolution near the domain boundaries and corners while maintaining good quality in the rest of the mesh. We further find that the stretching process has minimal impact on skewness but significantly increases aspect ratios and slightly reduces element quality. By fixing a specific stretch ratio index of  $l=5$ , we can generate meshes with varying resolutions while maintaining quality within acceptable CFD application standards.

#### Acknowledgment

This research was funded by the program Hibah Guru Besar, at Brawijaya University under contract number 4158.02/UN10.F09/PN/2023.

#### References

- [1] Hashim, Wan Alif Mustaqim Wan, Nurul Farhanah Azman, Mohamad Nor Musa, Syahrullail Samion, Nor Azwadi Che Sidik, and Yutaka Asako. "Air flow analysis and effect of angle on rotation vane blade through 90-degree by computational fluid dynamic." *Journal of Advanced Research in Fluid Mechanics and Thermal Sciences* 95, no. 2 (2022): 84-98. <https://doi.org/10.37934/arfmts.95.2.8498>
- [2] Taibi, R., G. Yin, and M. C. Ong. "CFD investigation of internal elbow pipe flows in laminar regime." In *IOP Conference Series: Materials Science and Engineering*, vol. 1201, no. 1, p. 012012. IOP Publishing, 2021. <https://doi.org/10.1088/1757-899X/1201/1/012012>

- [3] Mazumder, Quamrul H. "CFD analysis of the effect of elbow radius on pressure drop in multiphase flow." *Modelling and Simulation in Engineering* 2012 (2012): 37-37. <https://doi.org/10.1155/2012/125405>
- [4] Kumar, Shivam, Mukund Kumar, Samiran Samanta, Manoj Ukamanal, Asisha Ranjan Pradhan, and Shashi Bhushan Prasad. "Simulations of water flow in a horizontal and 90° pipe bend." *Materials Today: Proceedings* 56 (2022): 889-895. <https://doi.org/10.1016/j.matpr.2022.02.528>
- [5] Cao, Xuewen, Pan Zhang, Xiang Li, Zheng Li, Qianrong Zhang, and Jiang Bian. "Experimental and numerical study on the flow characteristics of slug flow in a horizontal elbow." *Journal of Pipeline Science and Engineering* 2, no. 4 (2022): 100076. <https://doi.org/10.1016/j.jpse.2022.100076>
- [6] Llorente, Ignacio M., Boris Diskin, and N. Duane Melson. *Plane smoothers for multiblock grids: Computational aspects*. No. NASA/CR-1999-209331. 1999.
- [7] Qian, Jian-Hua, Filippo Giorgi, and Michael S. Fox-Rabinovitz. "Regional stretched grid generation and its application to the NCAR RegCM." *Journal of Geophysical Research: Atmospheres* 104, no. D6 (1999): 6501-6513. <https://doi.org/10.1029/98JD02649>
- [8] Ali, Zaib, James Tyacke, Paul G. Tucker, and Shahrokh Shahpar. "Block topology generation for structured multi-block meshing with hierarchical geometry handling." *Procedia Engineering* 163 (2016): 212-224. <https://doi.org/10.1016/j.proeng.2016.11.050>
- [9] Ali, Zaib, and Paul G. Tucker. "Multiblock structured mesh generation for turbomachinery flows." In *Proceedings of The 22nd International Meshing Roundtable*, pp. 165-182. Cham: Springer International Publishing, 2014. [https://doi.org/10.1007/978-3-319-02335-9\\_10](https://doi.org/10.1007/978-3-319-02335-9_10)
- [10] Zhang, Yaixin, and Yafei Jia. "2D automatic body-fitted structured mesh generation using advancing extraction method." *Journal of Computational Physics* 353 (2018): 316-335. <https://doi.org/10.1016/j.jcp.2017.10.018>
- [11] Gupta, Murli M., and Jiten C. Kalita. "A new paradigm for solving Navier-Stokes equations: streamfunction-velocity formulation." *Journal of Computational Physics* 207, no. 1 (2005): 52-68. <https://doi.org/10.1016/j.jcp.2005.01.002>
- [12] Marchi, Carlos Henrique, Roberta Suero, and Luciano Kiyoshi Araki. "The lid-driven square cavity flow: numerical solution with a 1024 x 1024 grid." *Journal of the Brazilian Society of Mechanical Sciences and Engineering* 31 (2009): 186-198. <https://doi.org/10.1590/S1678-58782009000300004>
- [13] Moffatt, H. Keith. "A brief introduction to vortex dynamics and turbulence." In *Environmental Hazards: The Fluid Dynamics and Geophysics of Extreme Events*, pp. 1-27. 2011. [https://doi.org/10.1142/9789814313292\\_0001](https://doi.org/10.1142/9789814313292_0001)
- [14] Lintermann, Andreas. "Computational meshing for cfd simulations." *Clinical and Biomedical Engineering in the Human Nose: A Computational Fluid Dynamics Approach* (2021): 85-115. [https://doi.org/10.1007/978-981-15-6716-2\\_6](https://doi.org/10.1007/978-981-15-6716-2_6)
- [15] ANSYS. *ANSYS Meshing User's Guide*. ANSYS, Inc., 2020.